

## **Novel Tests of Gravity Below Fifty Microns**

Jeremy S. Johnson, Noah K. Dunkley, Gabriela D. Martinez, and Anthony E. Sanchez  
Department of Physics and Astronomy  
Humboldt State University  
One Harpst Street  
Arcata, California 95521 USA

Faculty Advisor: Dr. C.D. Hoyle

### **Abstract**

Theories which attempt to unify the Standard Model and General Relativity often include features which violate the Weak Equivalence Principle (WEP) and the gravitational Inverse-Square Law (ISL). A violation of either the WEP or the ISL at any length scale would bring into question our fundamental understanding of gravity. Motivated by these considerations, undergraduates and faculty at Humboldt State University are building an experiment to probe gravitational interactions below the 50-micron length scale. The experiment employs a torsion pendulum with equal masses of different material arranged as a “composition dipole.” We measure the twist of the torsion pendulum as an attractor mass is oscillated nearby in a parallel-plate configuration, providing a time varying torque on the pendulum. The size and distance dependence of the torque variation will provide a means to determine any deviations from either the WEP or the ISL at untested scales. This paper seeks to give a general overview of the experiment and to address recent improvements to the instrumentation involved, including the reduction of noise due to the environment and the reduction of uncertainty in the pendulum-attractor geometry.

**Keywords:** Gravity, Inverse-Square Law, Weak Equivalence Principle

### **1. Introduction**

Students and faculty at Humboldt State University (HSU) have been developing an experiment that will test the Weak Equivalence Principle (WEP) of General Relativity and the gravitational Inverse-Square Law (ISL) at unobserved distance scales. Roughly, the WEP states that the motion of a test mass under the influence of a gravitational field depends only on the mass of the objects involved. Tests of the WEP have been conducted with incredible precision over distances ranging from 1 cm to astronomical scales, all results being consistent with General Relativity. The ISL states that the force of gravity between two objects is proportional to the inverse-square of the distance between them. From previous experiments, the ISL has been found to be valid within experimental uncertainty from distances of  $\sim 50 \mu\text{m}$  to planetary scale. However, some models of Dark Energy, MOND, and String Theory predict that the ISL might fail over galactic distance scales or at very small separations.

### **2. Background and Motivation**

This research is prompted by numerous theoretical scenarios that attempt to combine the Standard Model and General Relativity. While General Relativity successfully describes gravity and has passed all experimental tests to date, it is inconsistent with the Standard Model of particle physics which describes the other three fundamental forces. Possible unification scenarios rely on additional spatial dimensions that could change the functional form of the ISL, providing

a potential source of experimental evidence for these scenarios<sup>1,2</sup>. Similarly, an observed violation of the WEP could give validation to possible unification schemes, pointing to new properties of gravity or evidence of new fundamental forces.

## 2.1 Inverse-Square Law

It is traditional to model deviations from the ISL by including a Yukawa addition<sup>3</sup> to the classical Newtonian potential energy. For point masses  $m_1$  and  $m_2$  separated by distance  $r$ , the gravitational potential energy equation becomes

$$V(r) = -\frac{Gm_1m_2}{r}(1 + \alpha e^{-r/\lambda}), \quad (1)$$

where  $G$  is the Newtonian gravitational constant,  $\alpha$  is a dimensionless scaling factor corresponding to the strength of any deviation relative to Newtonian gravity, and  $\lambda$  is the characteristic length scale where deviations might occur. For example, a value of  $\alpha$  equal to 1 would denote an interaction with strength equal to that of Newtonian gravity, with strength falling off via the exponential term. The goal of the experiment is to place constraints on these parameters.

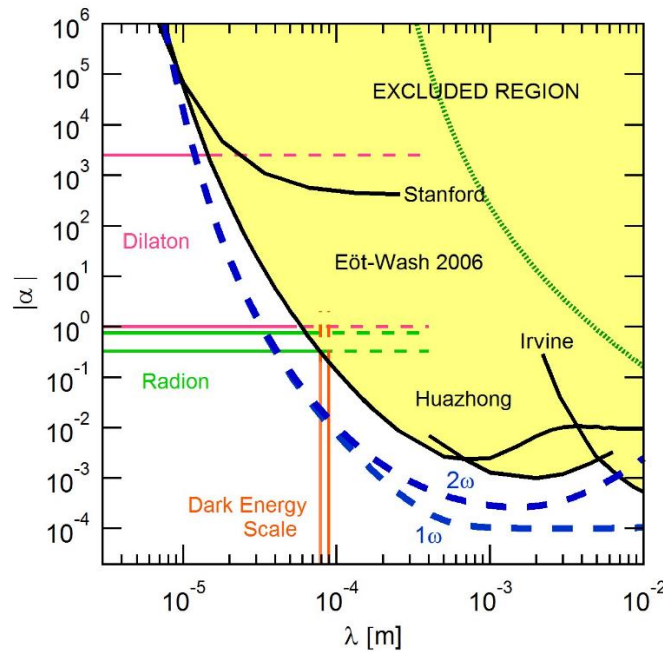


Figure 1. Current and predicted constraints on deviations from the ISL in Yukawa potential parameter space.

Figure 1 shows current constraints on deviations from the ISL in  $\alpha$ - $\lambda$  Yukawa parameter space. Possible deviations in the shaded region have been excluded at a 95% confidence level by previous experiments<sup>4,5,6,7</sup>. The blue dashed curves denoted the predicted sensitivity of the experiment at HSU. The difference between  $1\omega$  and  $2\omega$  is discussed in section 3. The green dashed curve denotes preliminary results from limited data; it is important to note that these constraints are not meant to be competitive but do show that our experiment is readily capable of measuring gravitational strength effects in the sub-cm regime. Other lines are various theoretical scenarios that may explain deviations if detected<sup>3</sup>.

## 2.2 Weak Equivalence Principle

Deviations from the WEP can be modeled in a similar way by introducing additional terms which characterize the composition of pendulums used in the experiment. A variation in the torque induced on a pendulum that is dependent

on composition and not on mass would hint at fundamentally new physics. With this consideration, the gravitational potential energy becomes

$$V(r) = -\frac{Gm_1m_2}{r} \left(1 + \tilde{\alpha} \left[ \frac{\tilde{q}}{g\mu} \right]_1 \left[ \frac{\tilde{q}}{g\mu} \right]_2 e^{-r/\lambda} \right), \quad (2)$$

where  $\mu$  is the mass of objects 1 or 2 in units of atomic mass units,  $u$ ,  $\tilde{g}$  is a coupling constant, and the  $\tilde{q}_i$  terms are “charges” that mediate possible new interactions. It is common to assume the parameterization

$$\tilde{q} = \tilde{g} \left[ Z \cos(\tilde{\psi}) + N \sin(\tilde{\psi}) \right], \quad (3)$$

where  $Z$  is the atomic number and  $N$  is the neutron number of the interacting materials, and  $\tilde{\psi}$  allows the charge to be an arbitrary linear combination of  $Z$  and  $N$ . Since baryon number is the sum of the atomic number and neutron number, while the lepton number is simply the atomic number for electrically neutral material, this parameterization allows for the investigation of interactions that couple to the seemingly conserved quantities of baryon number and lepton number.

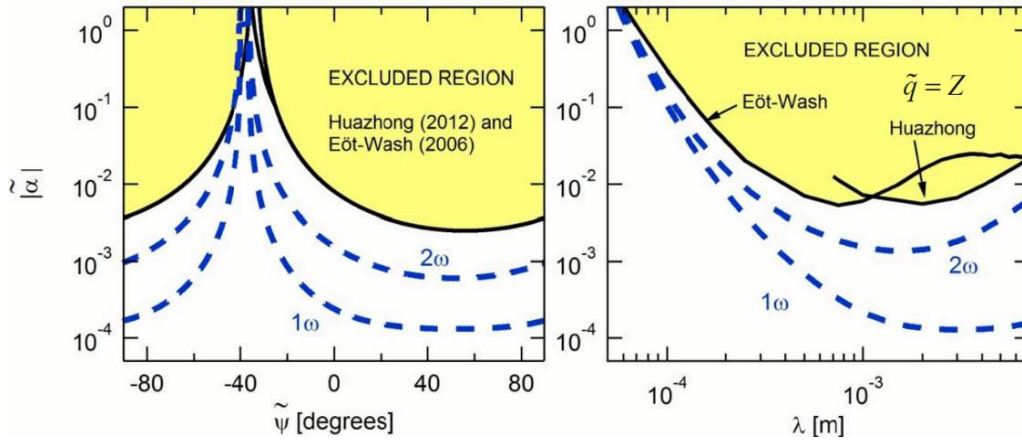


Figure 2. Current and predicted constraints on deviations from the WEP. Left:  $|\tilde{\alpha}|$ - $\tilde{\psi}$  plane assuming  $\lambda = 1$  mm. Right:  $|\tilde{\alpha}|$ - $\lambda$  plane assuming  $\tilde{\psi} = 0$ .

Similar to Figure 1, Figure 2 depicts current and predicted constraints on the WEP in Yukawa potential parameter space. It is important to note that we are now in a three-dimensional parameter space, denoting dependence on  $\alpha$ ,  $\lambda$ , and  $\psi$ , and that these plots, as well as that in Figure 1, are “slices” of the same parameter space.

### 3. Experimental Overview

The experiment is designed to measure the gravitational interaction between a stepped torsion pendulum and an attractor mass as their separation,  $s$ , is modulated at an angular frequency  $\omega$ . The modulation of the attractor mass provides a time varying torque on the pendulum, which can be measured via an optical system<sup>8</sup>. This signal is then analyzed and compared to the expected Newtonian torque to place constraints on the parameters described above.

Given that electromagnetic interactions would overwhelm any gravitational signal, the pendulum and attractor mass are separated by a  $20\mu\text{m}$ -thick BeCu foil which eliminates possible patch charge. Any time-dependent attractive force

due to the Casimir effect is also eliminated, since the distance between the pendulum and BeCu foil is constant. The pendulum-attractor geometry is housed in a vacuum chamber which is held at  $10^{-6}$ Torr to reduce viscous damping and thermal coupling to the pendulum. To further suppress thermal false effects, the vacuum chamber is held inside a thermally-isolated and temperature-controlled enclosure made of insulating Styrofoam sheets. For further discussion on various instrumentation used and possible false effects, see References [8,9,10].

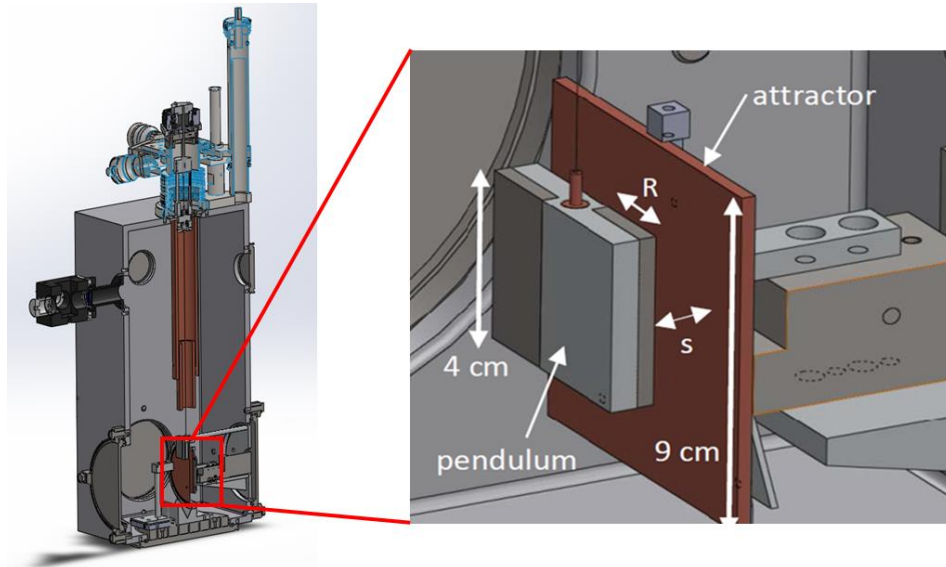


Figure 3. Left. CAD drawing of vacuum chamber. Right. Close-up of pendulum-attractor geometry. Note that BeCu foil is not shown in the right image.

The pendulum itself consists of an aluminum step and two titanium blocks (see Figure 3), and is hung using a  $25\mu\text{m}$ -diameter tungsten fiber. A null experiment, one in which the Newtonian torque is completely suppressed, could be achieved by employing an infinite plane attractor mass and noting that the gravitational force does not depend on  $s$ . This is approximated by using a relatively large attractor mass compared to the pendulum and noting that the attractor's gravitational force will not vary much over the thickness of the pendulum; thus the pendulum appears homogenous to Newtonian gravity. The geometry of the pendulum therefore enhances the effect due to possible short range interactions, since the pendulum appears inhomogeneous to these interactions.

As discussed above, the Newtonian signal is only present due to the finite size of the attractor mass, and predominantly occurs at  $1\omega$ . A short-range interaction, however, would cause a variation of the pendulum's twist at harmonics of the attractor modulation frequency, see Figure 4. Furthermore, systematic false effects are generally largest at  $1\omega$ <sup>8,9</sup>. This difference is evident in Figures 1 and 2; the curves denoted by  $2\omega$  are calculated independent of any signal at  $1\omega$  to show the experimental sensitivity in the case that the  $1\omega$  signal is unusable due to systematic false effects. Thus, while a signal at  $1\omega$  would be larger, signals at higher harmonics may be more reliable when determining new constraints. In practice, a combination of harmonics will be analyzed.

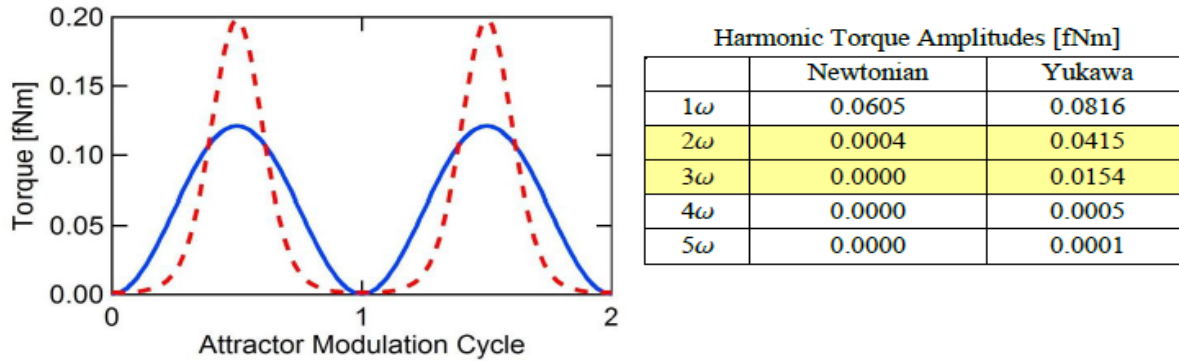


Figure 4. Left: Calculated Newtonian and possible Yukawa torques on the pendulum as a function of time for two attractor modulation cycles. Right: Table of harmonic torque amplitudes for the times series shown on the left.

For the torques depicted in Figure 4, the peak-to-peak distance modulation amplitude is 1 mm and the minimum separation is 100  $\mu\text{m}$ . Any Yukawa torque (red dashed curve) with  $\alpha = 1$  and  $\lambda = 100 \mu\text{m}$  would be clearly evident, and larger than the Newtonian background (blue solid curve). Notice that for the chosen parameters, the  $2\omega$  and  $3\omega$  Yukawa signals are clearly different from the tiny Newtonian torque amplitudes. This difference in frequency dependence can be used to place constraints on Yukawa parameters, while systematic effects that will be largest at  $1\omega$  can be largely avoided.

## 4. Experimental Progress

While the experiment is capable of producing and analyzing data it is not yet able to place new constraints on deviations, see Figure 1. Progress has been made to better characterize the separation distance between the pendulum and attractor-mass and to produce a more reliable parallel alignment of the pendulum-attractor-foil geometry. An active feedback (PID) system has been installed to suppress noise due to the apparatus tilt.

### 4.1 Linear Encoder

The movement of the attractor mass is controlled by a stepper motor using an eleventh order polynomial approximation to a sine wave and will have an amplitude of 0.5 mm. It is imperative when running our experiment to have precise knowledge of the position of our attractor mass relative to the pendulum, since knowledge of the minimum pendulum-attractor separation distance,  $s$ , is vital for estimating systematic errors.



Figure 5. Encoder read-head mounted on the stepper motor.

Using a vacuum-compatible optical encoder mounted onto the side of the motor, we are able to precisely determine the change in position as the attractor mass oscillates. The encoder read-head shines a collimated LED onto a gold plated scale which is reflected back onto the photo detector<sup>11</sup>. This produces two quadrature square wave signals with periods corresponding to 4 nm of movement, shown in Figure 6.

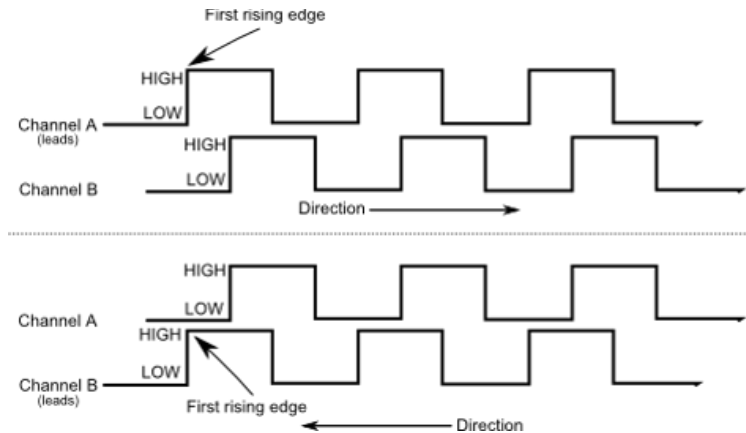


Figure 6. Quadrature Channels A and B<sup>12</sup>.

Figure 6 shows the two signals, A and B, obtained from the read-head. The signals are 90 degrees out of phase, which allows the encoder to obtain the direction of motion depending on which signal leads or lags. If the attractor mass moves right, channel A would lead channel B by 90 degrees. Motion to the left would correspond to channel B leading channel A by 90 degrees. The faster the attractor mass moves, the higher the frequency of both pulses. These square-wave signals are processed using a counter in LabVIEW, then converted into a position reading. This allows us to know the relative position with respect to the starting position of each data run, see Figure 7. Without such a device, we would have no knowledge of the exact position of the attractor.

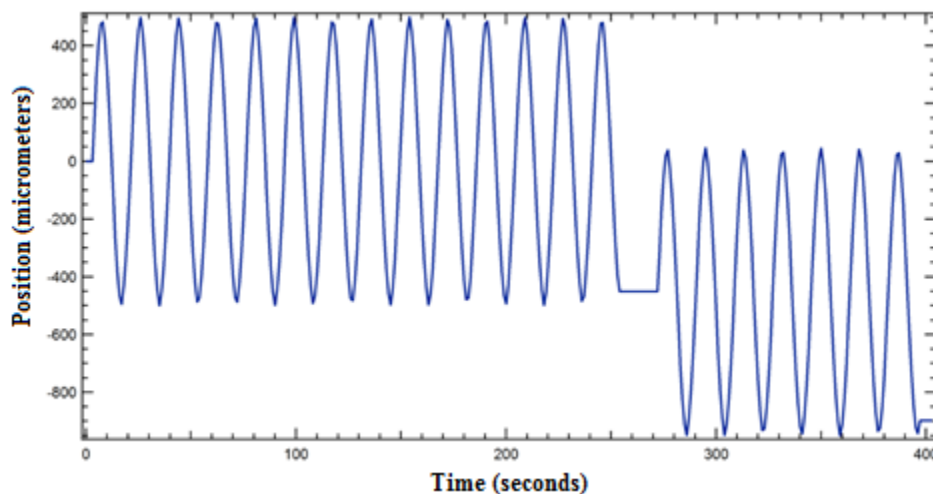


Figure 7. Sinusoidal motion of the attractor mass as a function of time as measured by the optical encoder.

Figure 7 demonstrates that the encoder system works and, perhaps more importantly, that the attractor's movement is what we expect. The "choppy" nature of the plot is due to the high frequency used during this test. In practice, the frequency will be a much smaller 0.005 Hz. The attractor's motion was stopped at around 250 seconds and resumed shortly after. Note, however, that the motion restarts, changing the point of oscillation. Furthermore, the encoder's data begins at  $0\mu\text{m}$ , independent of the attractor's real position. More steps must be taken in order for the encoder to record the attractor's *definitive* location, rather than only its relative motion. Future improvements to this system will include a reference marked scale which will help the encoder keep a set zero position for all data runs.

## 4.2 Capacitance Modeling

A reliable method of aligning the pendulum-attractor-foil geometry is important when attempting to achieve the desired minimum separation distance of about  $100\mu m$ . Furthermore, an offset of the pendulum and attractor-mass alignment is not accounted for when calculating the expected Newtonian torque and must be studied as a source of systematic error

A capacitance model can be used to determine the alignment and separation of the attractor-mass and foil membrane since, at a given separation, the capacitance between them will be minimized relative to any other orientation. Using a finite element analysis software (COMSOL), a 3-dimensional model is made using the material property constants of the attractor-mass and the foil membrane. This model can then be manipulated to any orientation and separation by modifying variables or by sweeping through a set of permutation of variables. Setting the attractor mass to high potential and the membrane assembly to ground, the software numerically calculates the capacitance between the two pieces in the model. Currently, the model only accounts for the attractor-mass and foil membrane. A future model will include the pendulum, attractor-mass assembly parts, and account for the vacuum chamber that surrounds assembly.

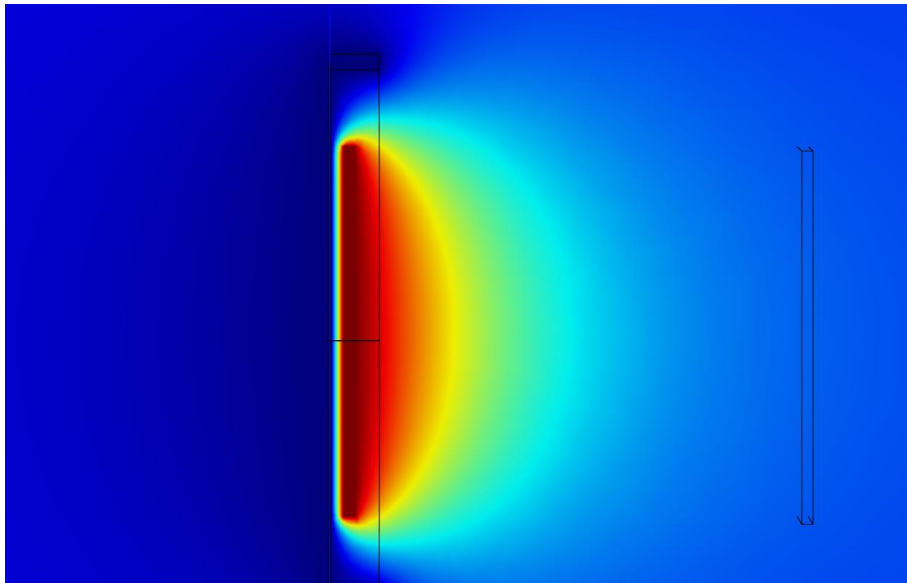


Figure 8. COMSOL electric potential plot for the attractor-mass and membrane assembly (denoted by the black lines in the red region). Dark red indicates high electric potential while blue indicates low electric potential. The lines on the right of the plot denote a “sweep” of the attractor mass and are otherwise irrelevant to the image.

## 4.3 Tilt Control

There is a measurable tilt of the apparatus due to movement of the building in which the experiment is located, see Figure 9. As the apparatus tilts, the separation distance,  $s$ , varies, potentially enhancing noise due to patch-charge interactions and introducing error in our knowledge of  $s$ . It is possible to decouple the vacuum chamber’s tilt from the building’s movement by employing an active feedback system to suppress the tilt; heating devices placed on the aluminum legs of the apparatus can change the length of each leg in such a way as to counteract any observed tilt. This is achieved using a PID loop that controls variable power supplies that drive the heaters.

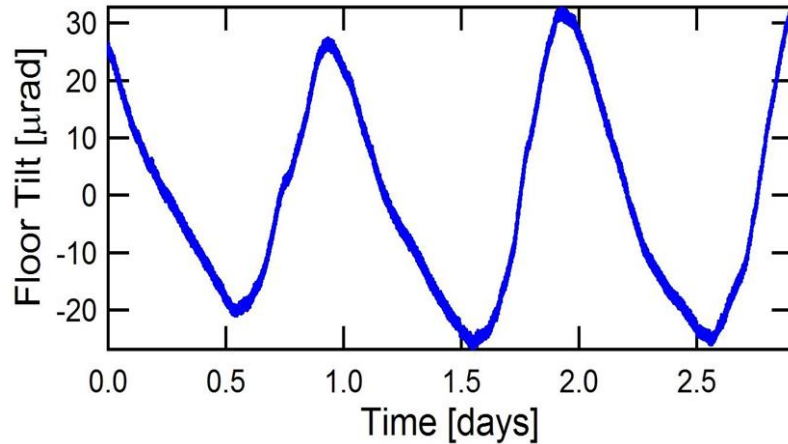


Figure 9. Tilt in one direction of the experiment with no correction. Note that the period of the tilt is one day.

This method has been tested to control tilt in the direction that affects s the most. The heating device is set at a baseline temperature which can then be further heated or cooled as determined digitally based on real-time data from tilt sensors on the apparatus.

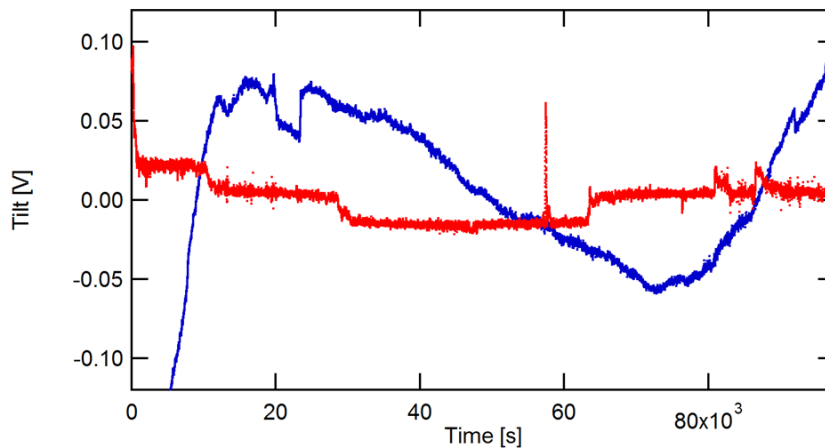


Figure 10. Tilt in one direction of the experiment through one day with correction (red) and without correction (blue). The vertical axis is proportional to the observed tilt ( $1V = 0.01$  degrees of tilt).

Preliminary tests show that the tilt can be reduced by at least a factor of 10 using this method. The spike in the corrected data is likely due to a slamming door or someone standing near the vacuum chamber; the “stepped” nature of the red curve is due to the power supply’s limited resolution. Further progress can be made by accounting for the other two legs and by using power supplies with greater resolution.

## 5. Conclusion

Students and faculty are developing an experiment at Humboldt State University that will probe the gravitational ISL and the WEP at untested distance scales. The novel parallel-plate torsion pendulum design will be the most sensitive apparatus to date for measuring gravitational effects below 50 microns. After taking preliminary data, progress has been made to better characterize important parameters and to suppress environmental noise. Preliminary data also indicate that the experiment is sensitive to gravitational-strength forces in the sub-cm regime. This sensitivity will be improved to the sub-mm level with further, improved data.



## 6. Acknowledgements

We are thankful for financial support from the National Science Foundation (grants PHY-1065697, PHY-1306783, and PHY-1606988), Research Corporation (Cottrell College Science Award CC6839), and the Humboldt State University College of Natural Resources and Sciences (CNRS), Sponsored Programs Foundation, and President's Office. Special thanks to Dr. C.D. Hoyle for the guidance we continue to receive in the Gravitational Research Laboratory.

## 7. References

1. N. Arkani-Hamed, S. Dimopoulos and G.R. Dvali, "New Dimensions at a Millimeter to a Fermi and Superstrings at a TeV," *Phys. Lett. B* **436**, 257 (1998).
2. G. Dvali, G. Gabadadze, M. Kolanovic and F. Nitti, "Scales of Gravity," *Phys. Rev. D* **65** (2001) 024031.
3. E.G. Adelberger, B.R. Heckel and A.E. Nelson, "Tests of the Gravitational Inverse-Square Law," *Ann. Rev. Nucl. Part. Sci.* **53** (2003) 77. [http://arxiv.org/PS\\_cache/hep-ph/pdf/0307/0307284v1.pdf](http://arxiv.org/PS_cache/hep-ph/pdf/0307/0307284v1.pdf)
4. D.J. Kapner, T.S. Cook, E.G. Adelberger, J.H. Gundlach, B.R. Heckel, C.D. Hoyle, and H.E. Swanson, "Tests of the Gravitational Inverse-Square Law below the Dark-Energy Length Scale," *Physical Review Letters* **98** 021101 (2007).
5. Andrew A. Geraci, Sylvia J. Smullin, David M. Weld, John Chiaverini, and Aharon Kapitulnik, "Improved constraints on non-Newtonian forces at 10 microns," *Physical Review D* **78**, 022002 (2008).
6. J. K. Hoskins, R. D. Newman, R. Spero, and J. Schultz, "Experimental tests of the gravitational inverse-square law for mass separations from 2 to 105 cm," *Physical Review D* **32**, 3084 (1985).
7. S.-Q. Yang, B.-F. Zhan, Q.-L. Wang, C.-G. Shao, L.-C. Tu, and W.-H. Tan, and J. Luo, "Test of the Gravitational Inverse Square Law at Millimeter Ranges," *Phys. Rev. Lett.* **108**, 081101 (2012). <http://link.aps.org/doi/10.1103/PhysRevLett.108.081101>
8. Leopardi, Holly . "Tests of Gravity Below Fifty Microns." *Proceedings of The National Conference On Undergraduate Research (NCUR) 2012*: 357-363. <http://www.ncurproceedings.org/ojs/index.php/NCUR2012/article/view/306/266> (accessed June 14, 2017).
9. Leopardi, Holly , and David Smith. "Short-Range Tests of Gravitational Physics ." *Proceedings of The National Conference On Undergraduate Research (NCUR) 2013*: 178-186. <http://www.ncurproceedings.org/ojs/index.php/NCUR2013/article/view/595/307> (accessed June 14, 2017).
10. Cardenas, Crystal, Andrew Harter, and Michael Ross. "Experimental Progress on Tests of Gravity at 20 microns." *Proceedings of The National Conference On Undergraduate Research (NCUR) 2014*: 811-819. <http://www.ncurproceedings.org/ojs/index.php/NCUR2014/article/view/927/569> (accessed June 14, 2017).
11. "How optical encoders work." *Renishaw*. <http://www.renishaw.com/en/how-optical-encoders-work--36979> (accessed June 15, 2017).
12. "Experiments in Quadrature Encoders." *Robotoid*. <http://www.robotoid.com/appnotes/circuits-quad-encoding.html> (accessed June 15, 2017).